Anesthesiology 2007; 107:756–67

Competitive Inhibition at the Glycine Site of the N-Methyl-D-aspartate Receptor by the Anesthetics Xenon and Isoflurane

Evidence from Molecular Modeling and Electrophysiology

Robert Dickinson, Ph.D., Brian K. Peterson, Ph.D.,† Paul Banks, B.Sc.,‡ Constantinos Simillis, M.B., B.S.,§ Juan Carlos Sacristan Martin, B.Sc.,‖ Carlos A. Valenzuela, Ph.D.,# Mervyn Maze, M.B., Ch.B.,** Nicholas P. Franks, Ph.D.††*

Background: **Inhibition of *N*-methyl-D-aspartate (NMDA) receptors by anesthetic gases and vapors may play an important role in anesthesia and neuroprotection. However, the site of action of these agents on the NMDA receptor is unknown. The authors show that xenon and isoflurane compete for the binding of the coagonist glycine on the NMDA receptor NR1 subunit.**

Methods: **Using a novel application of grand canonical Monte Carlo simulations, the authors predict the binding site of xenon on NMDA receptors. They test this prediction using electrophysiology on recombinant NMDA receptors.**

Results: **The authors' modeling predicts that xenon binds at the glycine site of the NMDA receptor. The authors show that inhibition of NMDA receptors by xenon and isoflurane increases as glycine concentration is decreased, consistent with the prediction of competitive inhibition at the glycine site. Lineweaver-Burk analysis shows that isoflurane inhibition seems purely competitive with glycine, but for xenon, there is an additional component of noncompetitive inhibition. The loss of inhibitory effect of xenon and isoflurane in mutant NR1(F639A)/NR2A receptors is explained by increased glycine affinity of the mutant receptors, and inhibition is restored at low glycine concentrations.**

Conclusions: **Xenon and isoflurane inhibit NMDA receptors by binding at the same site as the coagonist glycine. This finding may have important implications for general anesthesia and neuroprotection. Neuroprotectants that act at the glycine site of the NMDA receptor antagonists are well tolerated in patients, being devoid of psychotomimetic side effects, and the mechanism of inhibition may play a role in their clinical profile.**

This article is featured in "This Month in Anesthesiology." Please see this issue of ANESTHESIOLOGY, page 5A.

This article is accompanied by an Editorial View. Please see: Hemmings HC Jr: Noble meets nouveau: A shared anesthetic binding site for xenon and isoflurane on a glutamate receptor. ANESTHESIOLOGY 2007; 107:694–6.

Additional material related to this article can be found on the ANESTHESIOLOGY Web site. Go to http://www.anesthesiology.org, click on Enhancements Index, and then scroll down to find the appropriate article and link. Supplementary material can also be accessed on the Web by clicking on the "ArticlePlus" link either in the Table of Contents or at the top of the Abstract or HTML version of the article.

* Lecturer in Anaesthetics, ‡ Ph.D. Student, § Medical Student, ** Sir Ivan Magill Professor of Anaesthetics, †† Professor of Biophysics and Anaesthetics, Biophysics Section and Department of Anaesthetics, Pain Medicine and Intensive Care, Imperial College London, London, United Kingdom. † Research Associate, # Manager, Computational Modeling Centre, Air Products and Chemicals Inc., Allentown, Pennsylvania. ‖ R&D Manager, Medical Centre for Excellence, Air Products and Chemicals Inc., Madrid, Spain.

Received from the Biophysics Section, Imperial College London, London, United Kingdom. Submitted for publication April 17, 2007. Accepted for publication July 10, 2007. Supported by the Medical Research Council, London, United Kingdom; the Westminster Medical School Trust, London, United Kingdom; and Air Products and Chemicals Inc., Allentown, Pennsylvania. Mr. Banks received a studentship from the Westminster Medical School Trust. Drs. Franks and Maze have a financial interest in an Imperial College spin-out company (Protexeon Ltd., London, United Kingdom) that is interested in developing clinical applications for medical gases, particularly xenon, and both are paid consultants for this activity. Drs. Franks and Maze also sit on a Strategic Advisory Board that advises Air Products (Allentown, Pennsylvania) on possible medical applications for gases, including anesthetic gases.

Address correspondence to Dr. Dickinson: Blackett Laboratory, Imperial College London, South Kensington, London SW7 2AZ, United Kingdom. r.dickinson@imperial.ac.uk.

A CONSENSUS is emerging which suggests that general anesthetics act at ligand-gated ion channels at critical loci in the central nervous system (CNS),[1–3] and various criteria have been defined[2,4] to aid identification of putative ion channel targets. Three ligand-gated ion channels in particular have emerged as likely targets for a range of different anesthetics: the γ-aminobutyric acid type A receptor (etomidate, propofol, volatile agents), the glycine receptor (volatile agents), and the *N*-methyl-D-aspartate (NMDA) receptor (xenon, nitrous oxide, cyclopropane, ketamine). Although there is evidence that these channels are likely to be involved in general anesthesia, the molecular sites where anesthetics act on these channels have yet to be identified.

Many different approaches have been used to try to identify general anesthetic binding sites on ligand-gated ion channels, with varying degrees of success. The most widely used has been molecular biology combined with *in vitro* electrophysiology using recombinant expression systems, and this approach has identified critical determinants of anesthetic sensitivity for a variety of targets.[5–7] One drawback to this approach is that it is difficult, if not impossible, to tell whether the determinants form part of an anesthetic binding site or an allosteric site which "transduces" anesthetic binding into changes in gating. Direct approaches using x-ray protein crystallography have yet to be attempted, principally because of the absence of high-resolution crystal structures of ligand-gated ion channels. Nevertheless, in recent years, a number of high-resolution structures of extracellular domains of glutamate receptors have been published,[8,9] although no ion channel structures have been published that include a general anesthetic bound

to the protein. The recent publication of structures of ligand binding domains of the NMDA receptor,[9] and the unique structural simplicity of xenon suggested to us that a novel molecular modeling approach might be successful in identifying xenon binding sites on the NMDA receptor.

Antagonism of NMDA receptors may underlie xenon's anesthetic and analgesic actions[10,11] and may also play a role in its action as a neuroprotectant.[12] The NMDA receptor is one of the major classes of excitatory glutamate receptor found in the both the CNS and periphery and, currently, seven NMDA receptor subunits have been identified, NR1, NR2 (A–D), and NR3 (A and B). The precise stoichiometry of NMDA receptors is unclear, but it is thought likely that they are heterotetramers composed of two NR1 subunits plus two NR2 subunits and/or NR3 subunits. The agonists glycine and glutamate (or NMDA) bind to different subunits which interact allosterically to open the channel. The binding site for glycine is located on the extracellular domain of the NR1 subunit, whereas the binding site of glutamate (or NMDA) is located on the extracellular domain of the NR2 subunit.

To identify possible binding sites for xenon, we chose an approach involving grand canonical Monte Carlo (GCMC) simulations based on a published crystallographic structure of the NMDA receptor ligand binding domain.[9] GCMC simulations have been used to model the interactions of water and ligands with DNA[13] and have recently been used in the study of ligands binding to proteins.[14] To our knowledge, the use of GCMC simulations to model anesthetic binding sites on a ligand-gated ion channel has not previously been attempted. We first validated our model by successfully predicting known xenon binding sites on two proteins, previously identified using x-ray crystallography, before applying the method to the NMDA receptor. We then used the modeling procedure to look for xenon binding sites on the NMDA receptor, and this identified binding sites that overlapped with the glycine coagonist site. We tested the resulting prediction that xenon should compete for the binding of glycine using patch clamp electrophysiology on recombinant NMDA receptors expressed in HEK 293 cells. In addition, we also investigated the mechanism of inhibition of NMDA receptors by isoflurane, another anesthetic that inhibits NMDA receptors[11,15] and has been reported to have neuroprotective properties.[16]

Materials and Methods

Molecular Modeling

To identify potential sites for binding xenon, we used molecular simulations in the grand canonical ensemble.[17] In a GCMC simulation, the fixed parameters of the simulation are the chemical potential (μ_i), the volume (V), and the temperature (T). The number of molecules in the simulation cell varies *via* random insertion and destruction moves so as to maintain the chemical potentials at the specified value. We are primarily interested in finding plausible binding sites and not in extremely accurate representations of those sites, so for speed of computation, the protein is kept fixed and induced polarization is neglected as is usual.[18] These approximations are not a requirement, and a more complete treatment is possible.

We used a commercially available GCMC routine (Cerius2 Sorption Program; Accelrys, Inc., San Diego, CA) and force field.[19] The crystal structure of the NMDA receptor NR1 S1S2 ligand binding core[9] was retrieved from the protein data bank (structure code: 1PBQ). The unit cell contains two nonequivalent copies of the protein molecule that have slightly different degrees of domain closure. The structures were placed in a 65 Å × 65 Å × 110 Å simulation cell. The molecules of dichlorokynurenic acid (DCKA) were removed, hydrogens were added, and charge-balancing sodium ions were placed in the vicinity of the protein. GCMC simulation steps (40×10^6) were performed with temperature = 310°K and fugacities f_{Xe} = 1 bar and f_{H2O} = 0.5 kPa. Water is included such that the protein is hydrated but large numbers of water molecules do not fill the simulation cell and slow down the simulation. Coulomb interactions were calculated with Ewald sums, and the van der Waals interactions were summed to a cutoff radius of 12.5 Å. The relative probabilities of each type of Monte Carlo trial move were 2:1:1:1 for translation, rotation, creation, and destruction, respectively. After a 5×10^6–step equilibration period, every 5,000th configuration was saved to a trajectory file, and these were later analyzed with a clustering algorithm.

Clustering Analysis

Binding sites were determined *via* a clustering analysis (see appendix), detailed tests of which will be published elsewhere but which have been described in preliminary form.[20] Individual clusters contain xenon positions from the simulation which lie in regions that are relatively densely populated and which have favorable interaction energies. After the clusters are identified, their properties are determined. For the purposes of this work, we report the average and minimum energies of interaction, the occupancies of the clusters, and the probability that the clusters contain n xenon molecules, P(n). The xenon occupancy is defined as the weighted average of the number of xenon atoms in the cluster: $\text{occ} = \sum_{n=1}^{N} n\text{P}(n)$. The water occupancy of the xenon cluster is also reported.

Cell Culture and Transfection

HEK-293 cells (tsA201) were obtained from the European Collection of Cell Cultures (Salisbury, United King-

dom) and cultured using standard procedures. For electrophysiology, the cells were plated onto glass coverslips coated with poly-D-lysine. The culture medium was Dulbecco's modified Eagle's medium without glutamine, containing 400 μM DL-AP5 and 1 mM $MgCl_2$ to minimize excitotoxicity. Cells were transfected with complementary DNA (cDNA) using the calcium phosphate technique. The cDNA clones for rat NMDA receptor NR1-1a, NR2A, and NR2B subunits were kindly provided by Stephen F. Heinemann, B.S., Ph.D. (Professor, Molecular Neurobiology Laboratory, The Salk Institute for Biological Studies, San Diego, CA). NR1(F639A) mutant cDNA was made using the QuikChange II site-directed mutagenesis kit (Stratagene, La Jolla, CA) and confirmed by DNA sequencing (MWG Biotech, Ebersberg, Germany). Cells were cotransfected with green fluorescent protein for identification. Cells were used for electrophysiology 24–48 h after transfection.

Electrophysiology

Whole cell recordings were made using an Axoclamp 200B amplifier (Axon Instruments, Foster City, CA). Pipettes (3–5 MΩ) were fabricated from borosilicate glass and filled with internal solution containing 110 mM K-gluconate, 2.5 mM NaCl, 10 mM HEPES, and 10 mM BAPTA, titrated to pH 7.3 using KOH. The extracellular solution contained 150 mM NaCl, 2.5 mM KCl, 2 mM $CaCl_2$, and 10 mM HEPES, titrated to pH 7.35 using NaOH. Cells were voltage-clamped at −60 mV, and currents were filtered at 100 Hz (−3 dB) using an eight-pole Bessel filter (model 900; Frequency Devices Inc., Haverhill, MA), digitized (Digidata 1332A; Axon Instruments), and stored on a computer. Series resistance was compensated 75–90%. Data were acquired and peak currents measured using pClamp software (Axon Instruments). Solutions containing anesthetics were prepared as described previously.[11] Cells were exposed to NMDA and anesthetics using a rapid perfusion system.[21]

Data Analysis

Concentration–response curves for NMDA and glycine were fitted to the Hill equation: $y = I_{max} \times [agonist]^{n_H}/\{[EC_{50}]^{n_H} + [agonist]^{n_H}\}$, where n_H is the Hill coefficient. In the case of the glycine concentration–response curves for the NR1/NR2B and mutant NR1(F639A)/NR2A receptors, there was a small but measurable current even in the absence of added glycine. In these cases, the data were fit to a modified Hill equation with the addition of a fixed constant term y_0. For the analysis of competitive inhibition, Lineweaver-Burk (or double reciprocal) plots were used. Data were fit using a computer least squares regression program, with the data points weighted as the square of the rate.[22–24] The values of maximum rate, V_{max}, and K_M were obtained from the least squares regressions; the SEs in these parameters were calculated from the variance-covariance matrix. For mixed competitive and noncompetitive inhibition, the relative contributions of the competitive and noncompetitive sites can be calculated from the changes in K_M and V_{max}. In the presence of inhibitor, these become $K_M^* = (1 + i/K_c)\, K_M$ and $V^*_{max} = V_{max}/(1 + i/K_{un})$, where i is the concentration of inhibitor and K_c and K_{un} are the dissociation constants of the competitive and noncompetitive sites. Where P values are quoted, unless otherwise stated, we used a Student t test to assess significance.

Results

Molecular Modeling

To validate our molecular modeling procedure, we first performed simulations on protein structures with known xenon binding sites. We briefly describe below a test of the modeling procedure using the structure of cartilage oligomeric matrix protein (COMP; structure code 1VDF, World Wide Protein Data Bank, www.wwpdb.org). We retrieved the structure which contained no xenon and the structure of the xenon-containing derivative (V. N. Malashkevich, Ph.D., Department of Biochemistry, Albert Einstein College of Medicine, New York, personal communication, November 2003). The xenon derivative has eight xenon binding sites lying along the axis of the pore.[25] Our GCMC modeling successfully identified the eight xenon binding sites with a high predicted occupancy of approximately 0.9 (additional information regarding this is available on the ANESTHESIOLOGY Web site at http://www.anesthesiology.org). We also ran our simulations on the structure[26] of Phage T4 lysozyme L99A, another protein with known xenon binding sites, and our GCMC modeling successfully identified the xenon binding sites (data not shown; see Peterson *et al.*[20]).

Having validated the method, we ran GCMC simulations using the crystallographic structure of the S1S2 ligand binding core of the NR1 subunit of the NMDA receptor. In this structure (code 1PBQ), the crystallographic unit cell contains two copies of the S1S2 ligand binding core (chains A and B) that differ slightly in the degree of domain closure. Because the two copies of the protein are not identical, running the model on this structure effectively gave us two independent trials at modeling xenon binding sites.

The clustering analysis indicated only two superclusters with occupancies greater than 0.5. There was one site on each copy of the S1S2 ligand binding core, and both sites were in similar positions in each protein molecule (fig. 1A). From the clustering statistics, the binding sites are seen to be very similar, with approximately the same occupancies and energies of interaction (table 1). The sites had xenon occupancies of approximately 0.8 and 0.9, and in addition to xenon, the sites contained approximately 0.3 and 0.1 molecules of water, respectively. From the probability distribution (table 1), it can be seen that the binding sites exist in a variety of states

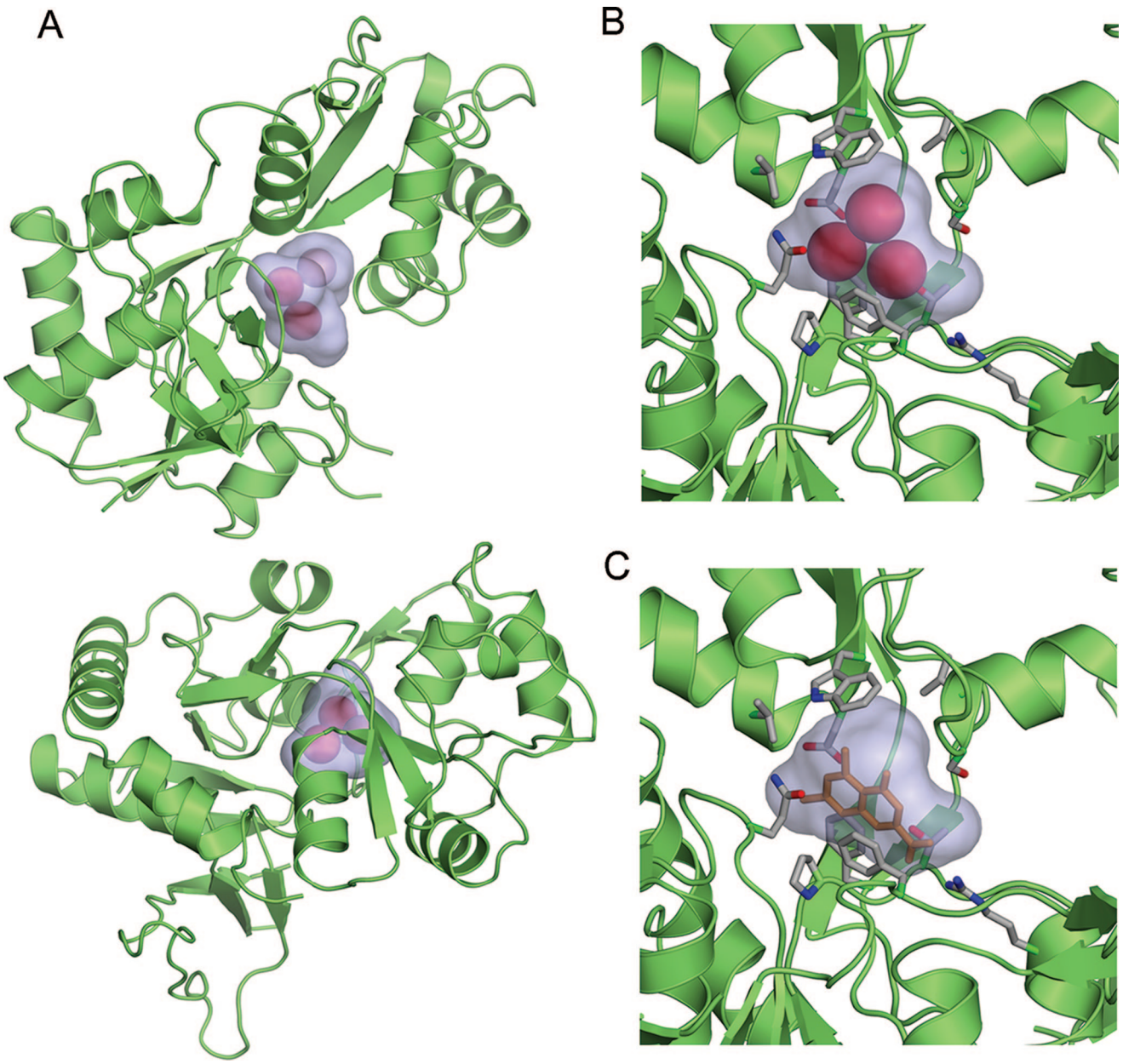

Fig. 1. (*A*) The crystal structure of the S1S2 ligand binding domain of the *N*-methyl-D-aspartate NR1 subunit showing the positions of the xenon binding sites predicted by our grand canonical Monte Carlo modeling. The published structure contains two nonidentical copies of the S1S2 domain (in different orientations), chain A (*lower panel*) and chain B (*upper panel*). The predicted xenon binding sites (superclusters) are represented by the *gray surfaces*. The *red spheres* represent xenon atoms at the center of the density clusters that comprise the binding sites. The predicted xenon binding sites are in equivalent positions in chains A and B, occupying the site normally occupied by glycine. (*B*) Crystal structure of the NR1 subunit showing the glycine binding site. The predicted xenon binding site in chain A is represented by the *gray surfaces*. The *red spheres* represent xenon atoms. The 11 amino acids identified from the modeling as being within 4 Å of the binding site (table 2) are shown as stick models (atoms color coded: *gray* = carbon; *blue* = nitrogen; *red* = oxygen). (*C*) The xenon atoms occupy the same position as the competitive inhibitor dichlorokynurenic acid, shown here as *orange sticks*. These images were produced using PyMol (PyMol Molecular Graphics System; DeLano Scientific, Palo Alto, CA).

of occupation, including being empty approximately one third of the time and containing up to three xenon atoms at other times.

The S1S2 ligand binding core consists of two domains that form a clamshell-like structure. The ligand glycine and the competitive inhibitor DCKA bind in the cleft between the two domains of the clamshell. Inspection of the images of the clusters (fig. 1) shows that they closely overlap with the glycine–DCKA binding sites. We next performed a contact analysis to determine which amino acids were within 4 Å of the minimum energy point of the clusters that make up the binding sites. These results are listed in table 2, and the residues are shown as stick models in figures 1B and C. Except for 1 residue (PHE 407 in chain B), the closest contacts are identical for each copy (chain A or chain B) of the protein. Of the 12

Table 1. GCMC Clusters in NMDA Receptor NR1 Ligand Binding Domain

Site No.	Xe Average Occupancy	H_2O Occupancy	E_{min}, kcal/mol	E_{avg}, kcal/mol	*P*(0)	*P*(1)	*P*(2)	*P*(3)
1	0.78	0.32	−6.69	−4.96	0.37	0.49	0.13	0.01
2	0.92	0.07	−6.48	−4.78	0.33	0.45	0.19	0.03

Only two sites with an average occupancy of more than 0.5 were identified. Sites 1 and 2 are equivalent sites on chains A and B of the protein corresponding to the glycine binding site of the *N*-methyl-D-aspartate (NMDA) receptor. The table shows the occupancy, the minimum (E_{min}) and average (E_{avg}) energy of the cluster, and the probability (*P*) that the site contains 0, 1, 2, or 3 xenon atoms. The occupancy is calculated from the weighted sum of these probabilities: $\text{occ} = \sum_{n=1}^{N} nP(n)$.

GCMC = grand canonical Monte Carlo; H_2O = water; Xe = xenon.

amino acids identified as making closest contacts with the xenon, the majority (6 in chain A and 7 in chain B) are apolar, 3 are polar (uncharged), and 2 are charged. Of the 12 amino acids we identify, 6 have been previously identified from the crystallographic structures[9] as being involved in interactions with glycine and 3 as being involved in interactions with DCKA (table 2).

Electrophysiology

Our prediction that xenon binds at the same site as glycine suggests that xenon may inhibit the NMDA receptor by competing with glycine. To test this, we performed competition experiments to measure the degree of inhibition of the receptor by xenon at different concentrations of agonist. If xenon binds at the same site as an agonist of the NMDA receptor, the degree of inhibition by xenon should increase as the concentration of that agonist is reduced. We chose to study NMDA receptors consisting of NR1/NR2A and NR1/NR2B subunits, the most prominent in adult hippocampus and neocortex.[27,28]

We first characterized the response of the different receptor subunit combinations to the agonist NMDA (in the absence and presence of xenon) at a fixed glycine concentration of 100 μM. The presence of 80% xenon inhibited the currents from both NR1/NR2A and NR1/NR2B receptors by approximately 30% without significantly changing the EC_{50} value for NMDA (figs. 2A and B). In the absence of xenon, the EC_{50} and n_H values for NMDA were 21 ± 3 μM and 1.1 ± 0.1, respectively, for NR1/NR2A receptors and 19 ± 4 μM and 1.0 ± 0.1 for NR1/NR2B receptors. In the presence of 80% xenon, the EC_{50} and n_H values for NMDA were 17 ± 2 μM and 1.3 ± 0.1, respectively, for NR1/NR2A receptors and 16 ± 2 μM and 1.0 ± 0.1 for NR1/NR2B receptors. Although there was a small decrease in the EC_{50} values for NMDA, this change was not significant (Student *t* test, $P > 0.05$). This indicates that the inhibition by xenon is not competitive at the NMDA binding site on the receptor (competitive inhibition would result in an *increase* in the EC_{50} value for NMDA). These findings are consistent with our earlier study on native NMDA receptors in hippocampal neurons.[10] There was no significant difference in the degree of inhibition by xenon for the different subunit combinations, with 80% xenon inhibiting the receptors by 30 ± 2% and 33 ± 1% for NR1/NR2A and NR1/NR2B receptors, respectively (Student *t* test, $P > 0.05$; fig. 2C).

Having established that the inhibition by xenon was not competitive with NMDA, we investigated whether xenon was competitive with the coagonist glycine as suggested by our modeling. We also investigated the effects of isoflurane. We chose the volatile agent isoflurane because of its widespread clinical use and also because of conflicting reports in the literature as to the sensitivity of NMDA receptors to isoflurane.[11,15,29,30] Although we did not model isoflurane binding to the NMDA receptor, we did confirm that an isoflurane molecule would fit in the xenon binding site identified by our GCMC simulations (additional information regarding this is available on the ANESTHESIOLOGY Web site at http://www.anesthesiology.org). To determine whether xenon and isoflurane compete with glycine, we measured the inhibition by these agents at a series of different glycine concentrations for each of the receptor combinations.

Figure 3A shows the concentration–response curve for glycine for the NR1/NR2A receptors. The EC_{50} and n_H for glycine are 5.7 ± 1.5 μM and 0.8 ± 0.2, respectively. We then measured the inhibition of the NR1/NR2A receptors by 80% xenon at different glycine concentrations (fig. 3B). We found that, as the glycine concentration was reduced, the inhibition by xenon increased. At a glycine concentration of 100 μM, 80% xenon inhibited

Table 2. Amino Acid Residues within 4 Å of the Identified Xenon Binding Sites

Site No.	Amino Acid Residue No.					
1 (Chain A)	GLN405*	PHE484†	PRO516*	THR518*	ARG523*	
	SER688*	VAL689	TRP731*†	ASP732*	VAL735	PHE758
2 (Chain B)	GLN405*	PHE408†	PHE484†	PRO516*	THR518*	ARG523*
	SER688*	VAL689	TRP731*†	ASP732*	VAL735	PHE758

* Interacts with glycine. † Interacts with dichlorokynurenic acid. From crystallographic data.[9]

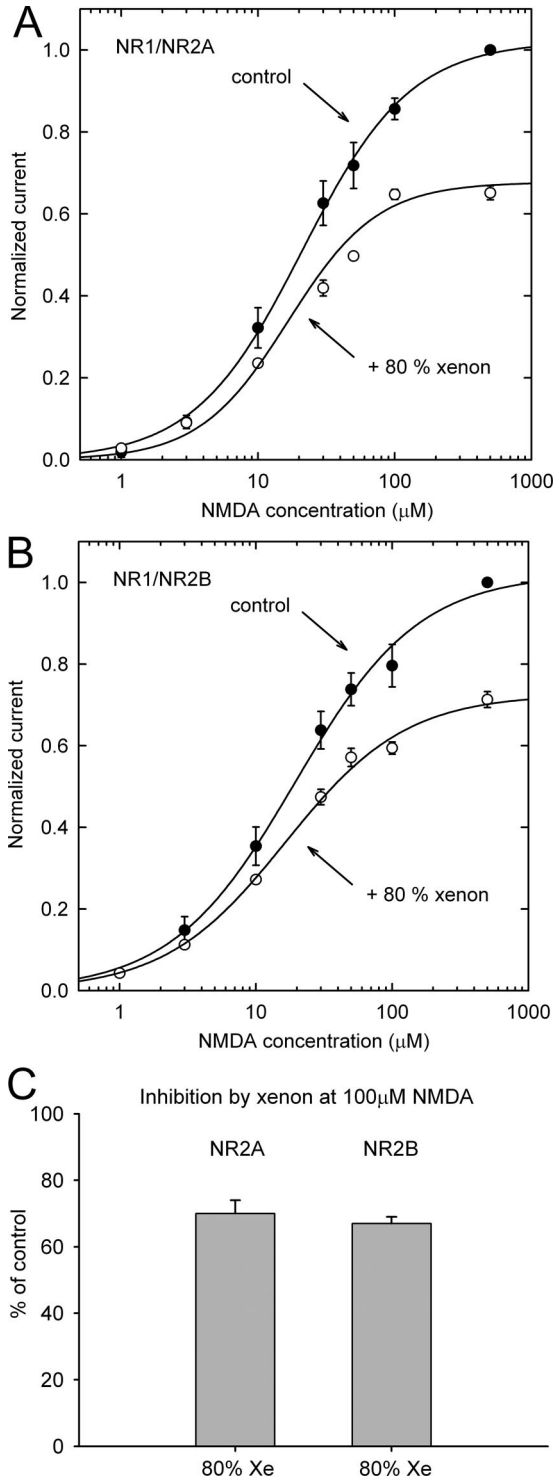

Fig. 2. Concentration–response curves for activation of receptors by *N*-methyl-D-aspartate (NMDA) in the absence (●) and presence (○) of 80% xenon for NR1/NR2A receptors (*A*) and NR1/NR2B receptors (*B*). The concentration of the coagonist glycine was 100 μM throughout. Each *point* represents the mean value from, on average, 7 cells (NR2A), or 6 cells (NR2B). The *error bars* are SEs; where not shown, these are smaller than the symbol. The curves are fitted to the Hill equation, as described in the text. (*C*) There was no significant difference ($P > 0.05$) in the inhibition of NR1/NR2A or NR1/NR2B receptors by 80% xenon (Xe). The data shown are at an NMDA concentration of 100 μM. The values are means from 11 cells (NR2A) and 8 cells (NR2B). The *error bars* are SEs.

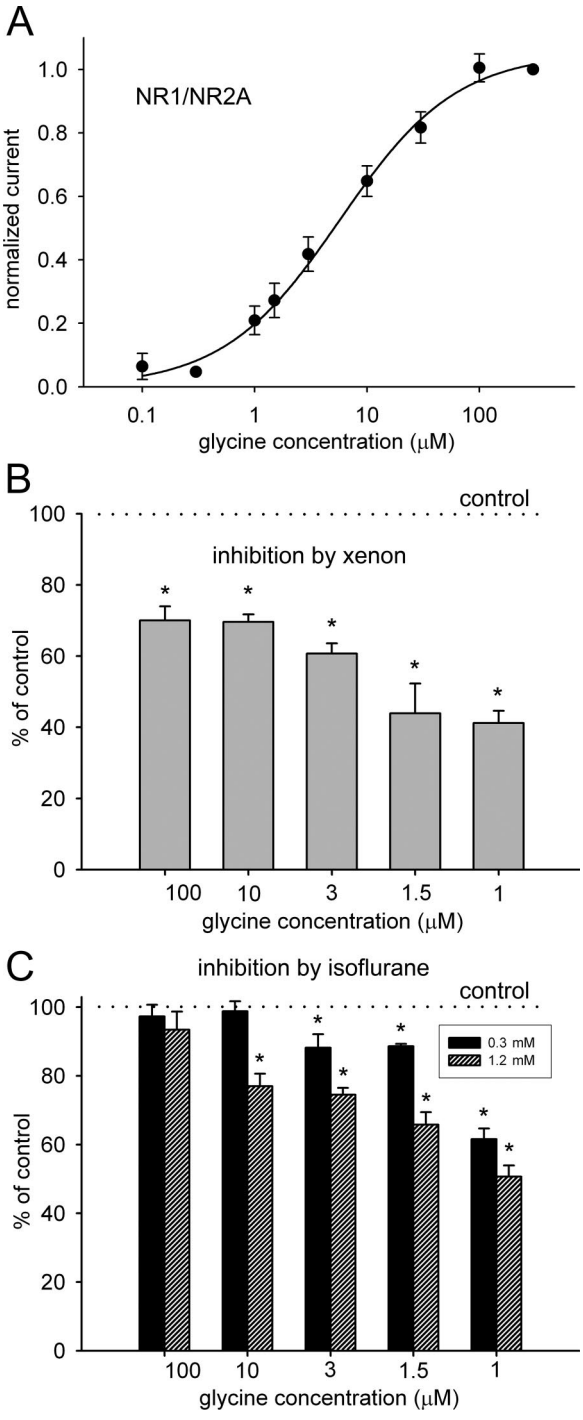

Fig. 3. (*A*) Glycine concentration–response curve for activation of NR1/NR2A receptors at a concentration of 100 μM *N*-methyl-D-aspartate. The curve is fitted to the Hill equation. The *points* represent mean values from 8 cells. The *error bars* are SEs; where not shown, these are smaller than the symbol. (*B*) Xenon (80%) inhibition of NR1/NR2A receptors increases as glycine concentration is reduced. (*C*). Inhibition of NR1/NR2A receptors by 0.3 mM (1 minimum alveolar concentration [MAC]) isoflurane (*black bars*) and 1.2 mM (4 MAC) isoflurane (*cross-hatched bars*) increases as glycine concentration is reduced. The *bars* represent mean values from an average of 8 cells (xenon) or 7 cells (isoflurane) at each glycine concentration. The *error bars* are SEs. * Significantly different ($P < 0.05$) from control (100%), indicated by *dashed line*.

the currents by 29 ± 1%. However, at lower glycine concentrations, the inhibition increased significantly, reaching 59 ± 5% at 1 μM glycine (Student *t* test, $P < 0.01$, compared with 100 μM). This is consistent with our prediction that xenon competes for binding of glycine at the glycine binding site.

When we tested isoflurane at the clinically relevant concentration of 0.3 mM [31] (equivalent to 1 MAC = minimum alveolar concentration for anesthesia) on the NR1/NR2A combination at 100 μM glycine, the receptors were insensitive to isoflurane with only 2.7 ± 0.1% inhibition (fig. 3C). Increasing the isoflurane concentration to 1.2 mM (equivalent to 4 MAC) resulted in only 6.6 ± 0.4% inhibition at 100 μM glycine (fig. 3C). However, at a lower glycine concentration of 1 μM, isoflurane inhibited strongly, with 1 MAC isoflurane inhibiting by 38 ± 2% and 4 MAC isoflurane inhibiting by 49 ± 3% (fig. 3C). The change in isoflurane sensitivity between the high (100 μM) and low (1 μM) glycine concentrations was even more marked than in the case of xenon, consistent with isoflurane also competing for glycine at the glycine binding site.

The concentration–response curve for glycine for the NR1/NR2B receptor is shown in figure 4A. The NR1/NR2B receptor has a 10-fold higher affinity for glycine compared with the NR1/NR2A receptor. For the NR1/NR2B receptors, the EC_{50} for glycine is 0.58 ± 0.19 μM and the n_H is 0.7 ± 0.2. We measured the inhibition of the NR1/NR2B receptors by 80% xenon at different glycine concentrations (fig. 4B). We found that, as the glycine concentration was reduced, the inhibition by xenon increased in a similar manner to the NR1/NR2A receptors. At a high glycine concentration (100 μM), 80% xenon inhibited the currents by 33 ± 1%. However, at lower concentrations of glycine, the inhibition increased, with 80% xenon inhibiting by 57 ± 7% at 0.03 μM glycine (Student *t* test, $P < 0.01$, compared with 100 μM).

A similar pattern was observed with isoflurane inhibition of the NR1/NR2B subunit combination (fig. 4C). At high glycine (100 μM), the NR1/NR2B receptors were inhibited by isoflurane somewhat more than the NR1/NR2A receptors (fig. 4C), although the inhibition was modest, with 14.6 ± 0.4% inhibition at 1 MAC isoflurane and 33 ± 1% at 4 MAC isoflurane. However, as the glycine concentration was reduced, the inhibition increased, with isoflurane inhibiting by 36 ± 3% and 58 ± 7% at 1 and 4 MAC, respectively, at a glycine concentration of 0.03 μM (fig. 4C). Our findings that inhibition by xenon and isoflurane increases at low glycine concentration for both NR1/NR2A and NR1/NR2B subunit combinations suggest that both anesthetics inhibit NMDA receptors by binding at the glycine site and competing for glycine.

To quantify the degree of competitive inhibition, we constructed Lineweaver-Burk plots (fig. 5) for isoflurane and xenon inhibition of the NMDA receptors. From the

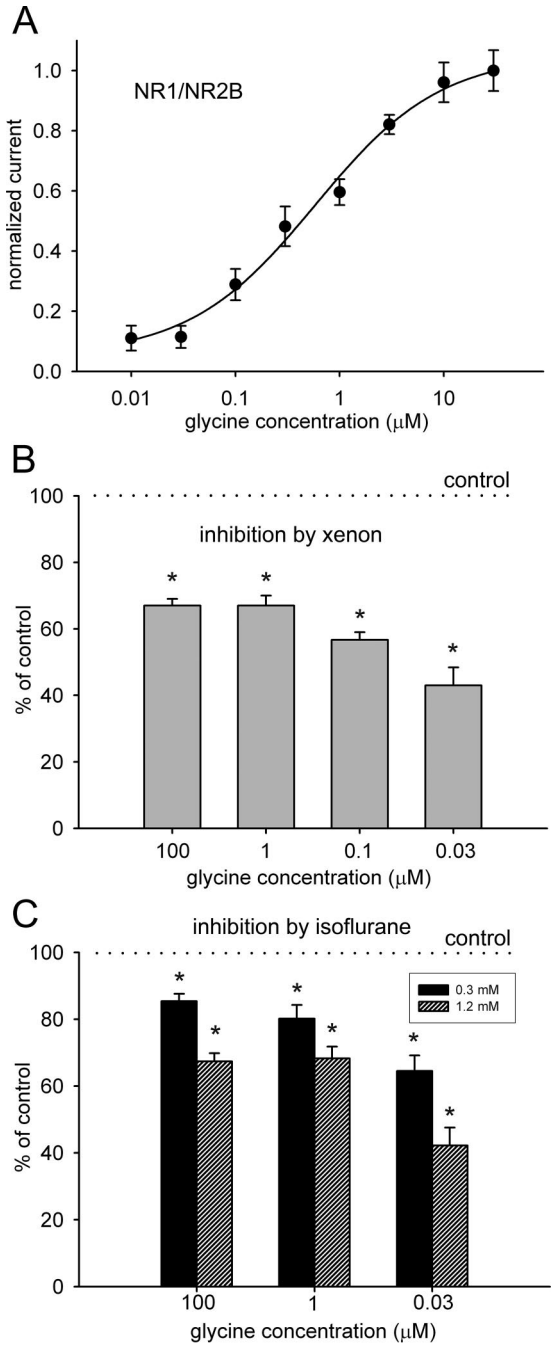

Fig. 4. (*A*) Glycine concentration–response curve for activation of NR1/NR2B receptors at a concentration of 100 μM *N*-methyl-D-aspartate. The curve is fitted to the Hill equation. The *points* represent mean values from 8 cells. (*B*) Xenon (80%) inhibition of NR1/NR2B receptors increases as glycine concentration is reduced. (*C*) Inhibition of NR1/NR2B receptors by 0.3 mM (1 minimum alveolar concentration [MAC]) isoflurane (*black bars*) and 1.2 mM (4 MAC) isoflurane (*cross-hatched bars*) increases as glycine concentration is reduced. The *bars* represent mean values from an average of 7 cells (xenon) or 4 cells (isoflurane) at each glycine concentration. *Error bars* are SEs. * Significantly different ($P < 0.05$) from control (100%), indicated by *dashed line*.

Lineweaver-Burk plot for the NR1/NR2A control data, the value of the K_M for glycine is 3.9 ± 0.3 μM, and the maximum rate, V_{max}, is 0.98 ± 0.03. In the case of isoflurane (fig. 5A), the Lineweaver-Burk plot indicates

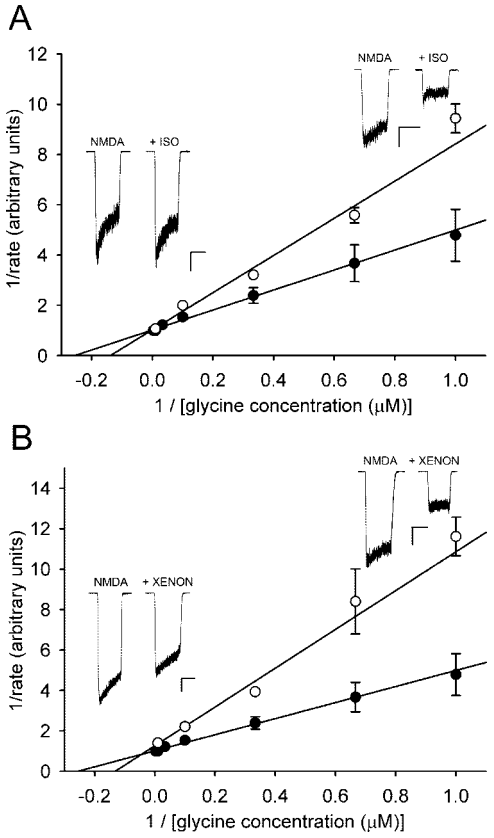

Fig. 5. (*A*) Lineweaver-Burk plot showing competitive inhibition by isoflurane. The *points* show data in the absence (●) and presence (○) of 1.2 mM isoflurane (ISO) for the NR1/NR2A receptor. From the control data, the value of the K_M and maximum rate, V_{max}, are 3.9 ± 0.3 μM and 0.98 ± 0.04, respectively. In the presence of isoflurane, the K_M increases to 7.6 ± 1.5 μM, whereas V_{max} is unchanged (0.99 ± 0.12). (*B*) Lineweaver-Burk plot showing mixed competitive and noncompetitive inhibition by xenon. The *points* show data in the absence (●) and presence (○) of 80% xenon for the NR1/NR2A receptor. From the control data, the K_M and V_{max} are 3.9 ± 0.3 μM and 0.98 ± 0.04, respectively. In the presence of xenon, the K_M increases to 7.1 ± 1.3 μM, whereas V_{max} decreases to 0.78 ± 0.09. The *points* represent means from 8 cells (control and xenon) or 7 cells (isoflurane). The *error bars* are SEs; where not shown, these are smaller than the symbol. The *lines* are least square regressions, weighted as described in the text. The *insets* show representative traces in the absence and presence of 1.2 mM isoflurane (*A*) or 80% xenon (*B*) at glycine concentrations of 100 μM (*lower left*) and 1 μM (*upper right*). The *horizontal* and *vertical scale bars* represent 5 s and 150 pA, respectively. NMDA = *N*-methyl-D-aspartate.

purely competitive behavior, as shown by the fact that in the presence of anesthetic, there was no change in V_{max} (0.97 ± 0.11) but there was a significant increase in the apparent K_M for glycine to 7.2 ± 1.2 μM ($P < 0.01$, Student *t* test). However, in the case of xenon, the Lineweaver-Burk plot (fig. 5B) indicated mixed competitive and noncompetitive inhibition, as shown by both a significant decrease in V_{max} to 0.79 ± 0.09 ($P < 0.025$, Student *t* test) and an significant increase in the apparent K_M for glycine to 7.58 ± 1.26 μM ($P < 0.01$, Student *t* test). To determine the relative contributions of the competitive and noncompetitive components of inhibition by xenon, we used the changes in K_M and V_{max} to estimate the relative values of the inhibition constants (K_i) for the competitive and the noncompetitive sites. The K_i for the competitive site is estimated to be approximately 3.9-fold lower than that for the noncompetitive site, indicating that at low glycine concentration, xenon will bind preferentially at the glycine site compared with the noncompetitive site.

It has recently been reported[30] that a mutation (F639A) in the second transmembrane domain (TM2) of the NR1 subunit reduces (but does not eliminate) inhibition by xenon, and almost completely abolishes inhibition by 1 MAC isoflurane. To investigate whether this is consistent with our finding that these anesthetics are competitive inhibitors at the glycine site, we studied mutant NR1(F639A) receptors. We first determined the sensitivity of the NR1(F639A)/NR2A receptors to glycine. The glycine concentration–response curve for the NR1(F639A)/NR2A receptors is shown in figure 6A. The EC_{50} and n_H for glycine are 1.4 ± 0.2 μM and 0.9 ± 0.1, respectively. Compared with the wild-type NR1/NR2A receptors, the NR1(F639A) mutant receptors are fourfold more sensitive to glycine. An obvious consequence of this is that a given concentration of glycine represents a different point on the concentration–response curve of the mutant or wild-type receptor. The inhibition by isoflurane of the wild-type and NR1(F639A)/NR2A receptors is shown in figure 6B. At a concentration of 1 μM glycine, the wild-type receptors are inhibited by 38 ± 2% and 49 ± 3% at 1 and 4 MAC isoflurane, whereas the mutant NR1(F639A)/NR2A receptors are much less sensitive, with inhibitions of only 8.1 ± 0.4% and 8.6 ± 0.1% at 1 and 4 MAC isoflurane, respectively. However, it is clear from figure 6A that although 1 μM glycine represents a "low" concentration for the wild type receptors, it is close to the EC_{50} concentration for the NR1(F639A)/NR2A receptors. We therefore investigated whether the inhibition by isoflurane of the mutant receptors increased when the glycine concentration was reduced, as we had observed for the wild-type receptors. At a lower concentration of 0.03 μM glycine, the NR1(F639A)/NR2A receptors were inhibited by 38 ± 4% and 64 ± 9% at 1 and 4 MAC isoflurane, respectively (fig. 6B). We observed similar behavior with xenon (fig. 6C). At a concentration of 1 μM glycine, the wild-type receptors were inhibited by 59 ± 5% at a concentration of 80% xenon, whereas the mutant NR1(F639A)/NR2A receptors are less sensitive with inhibitions of 15.1 ± 0.6% at 80% xenon. However, when the glycine concentration was reduced to 0.03 μM, the inhibition of the NR1(F639A)/NR2A receptors by 80% xenon increased to 40 ± 1%. Hence, the apparent reduction in sensitivity to isoflurane and xenon of the mutant NR1(F639A)/NR2A receptors compared with the wild-type receptors at 1 μM glycine can be explained by the leftward shift of the glycine concentration–response curve for the mutant receptor (fig. 6A).

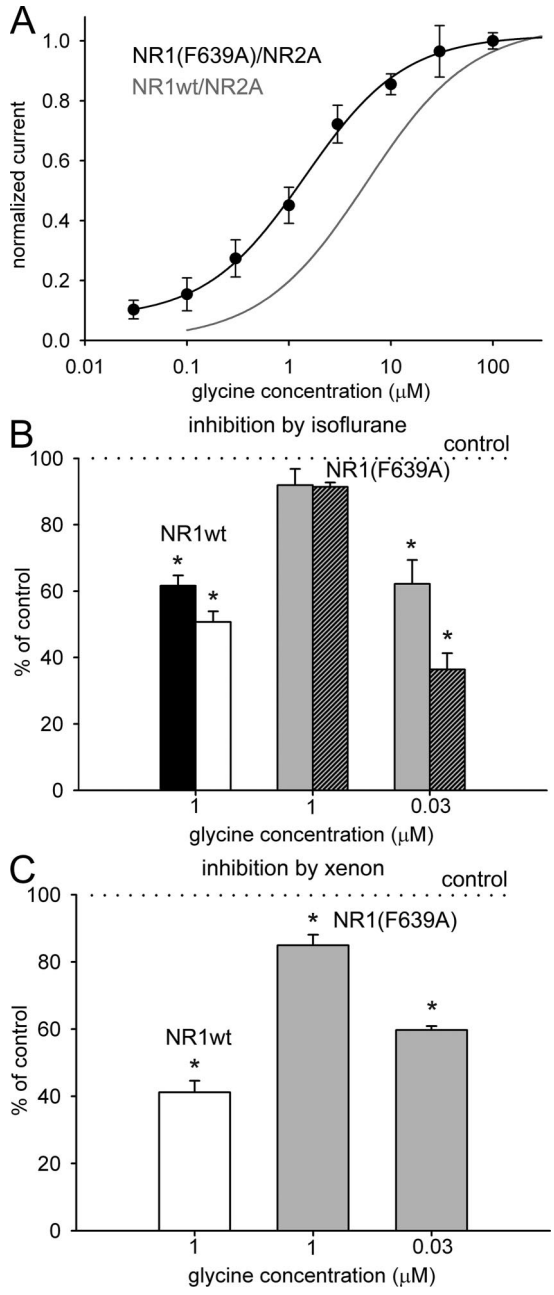

Fig. 6. (*A*) Glycine concentration–response curve for activation of mutant NR1(F639A)/NR2A receptors at a concentration of 100 μM *N*-methyl-D-aspartate. The curve is fitted to the Hill equation. The *points* represent mean values from an average of 6 cells at each concentration. For comparison, the glycine concentration–response curve for the wild-type NR1/NR2A receptors (NR1wt) is shown in *gray*. (*B*) At a glycine concentration of 1 μM, the wild-type receptors are inhibited at 1 minimum alveolar concentration (MAC) (*black bar*) and 4 MAC (*white bar*) isoflurane, respectively. At 1 μM glycine, the NR1(F639A)/NR2A receptors are less sensitive to 1 MAC isoflurane (*gray bar*) and 4 MAC isoflurane (*cross-hatched gray bar*). Isoflurane inhibition of NR1(F639A)/NR2A receptors is restored at a 0.03 μM glycine. (*C*) At a glycine concentration of 1 μM, xenon (80%) inhibits the wild-type receptors (*white bar*). At 1 μM glycine, the NR1(F639A)/NR2A receptors are less sensitive to 80% xenon (*gray bar*). Xenon (80%) inhibition (*gray bar*) of NR1(F639A)/NR2A receptors increases at 0.03 μM glycine. The *bars* are means for an average of 6 cells at each concentration. *Error bars* are SEs. * Significantly different ($P < 0.05$) from control (100%), indicated by *dashed line*.

Discussion

Modeling

The prediction that xenon binds to the NMDA receptor at the same site as the ligand glycine was unexpected. The idea that anesthetics might act by competitive inhibition of receptors was first proposed more than 20 yr ago.[23] However, at that time there was little information on the effects of anesthetics on CNS ion channels. Our GCMC modeling technique successfully predicts known xenon binding sites on COMP, and our simulations on the NMDA receptor predict that xenon binds at the same site as glycine. Furukawa and Gouaux[9] propose that the binding of glycine results in a closure of the S1S2 ligand binding domain leading to gating of the receptor and opening of the ion channel. They propose that the inhibitor DCKA prevents gating of the channel by stabilizing a more open conformation of the ligand binding core. Our modeling predicts that xenon occupies the same position as DCKA (fig. 2B). Hence, it is possible that the competitive component of xenon inhibition may be due to xenon stabilizing the more open conformation of the domains, thus inhibiting the opening of the ion channel, in a similar manner to DCKA.

Electrophysiology

Since our first demonstration that xenon potently inhibited NMDA receptors[10] in hippocampal neurons, other studies have reproduced the finding using recombinant expression systems.[29,32] However, the degree of inhibition by xenon reported (approximately 30–40%) was somewhat less than we observed in hippocampal neurons (approximately 60%). Our finding that xenon inhibition is competitive with glycine provides an explanation for the discrepancies in the degree of inhibition reported. Our original experiments on neurons were performed at 1 μM glycine, whereas the other studies have used higher concentrations of glycine. The results presented here show that reducing the glycine concentration can increase the degree of inhibition by 80% xenon from approximately 30% to 60%.

A number of studies of the effects of isoflurane on NMDA receptors have reported varying inhibition by clinical concentrations of isoflurane.[11,15,33] As discussed above, the different degrees of inhibition by isoflurane may be due to different glycine concentrations being used.

It should be noted that many electrophysiologic studies (including our own) have been performed in conditions that differ slightly from that found physiologically, perhaps the most obvious of which is the lack of magnesium. Magnesium is a voltage-dependent channel blocker. Under resting physiologic conditions, NMDA receptors are blocked by magnesium. However, when the cell is depolarized (*e.g.*, by an action potential), magnesium block is removed, allowing the NMDA recep-

tor to function as a coincidence detector. It should be borne in mind, therefore, that the inhibition of NMDA receptors by anesthetics would be observed physiologically when the postsynaptic cell is depolarized.

Competitive versus *Noncompetitive Inhibition*

Our electrophysiologic studies with xenon support the modeling prediction that xenon binds at the same site as glycine on the NMDA receptor. However, in addition to competitive inhibition at the glycine site, our results show that there is also a component of noncompetitive inhibition. The nature of the noncompetitive site remains to be elucidated. It is possible that in addition to binding at the glycine site, xenon also interacts with other domains of the NR1 subunit and/or the NR2 subunit to inhibit the NMDA receptor in a noncompetitive manner. In comparing the inhibition by isoflurane and xenon, one obvious difference is that the inhibition by isoflurane seems to be purely competitive (fig. 5A). There have been conflicting reports in the literature regarding the sensitivity of NMDA receptors to isoflurane, with some studies reporting that they are sensitive, whereas others have reported a lack of sensitivity. Our finding that isoflurane inhibition is competitive with glycine now provides an explanation for the discrepancy. Many studies have used fixed (and different) glycine concentrations. Hence, the differing degrees of inhibition reported in different studies may well be due to the different glycine concentrations used.

Mutational Studies

Our modeling studies identified 12 amino acids (table 2) within 4 Å of the positions of xenon atoms. At first sight, it may seem that an obvious experiment is to mutate these residues with the idea that this may disrupt the binding of xenon, confirming our prediction. However, the situation is confounded by the fact that xenon binds at the same site as glycine. Many of the identified residues are known to interact with glycine.[9] Indeed, mutations in the glycine binding site have been extensively studied (for a review, see Dingledine *et al.*[34]) and can cause large changes (>1,000-fold) in glycine affinity. It is highly likely that mutating a residue in the glycine binding site will have a critical affect on the binding of glycine.

The recent observation[30] that a mutation (F639A) in TM2 of the NR1 subunit reduces inhibition by xenon and isoflurane, suggested to us an alternative approach. Given that this amino acid in TM2 is distant from the glycine binding site, this result might seem to be at odds with our finding of competitive inhibition at the glycine site. However, we have shown that the F639A mutation increases the glycine affinity of the NMDA receptor fourfold compared with the wild-type receptors and that the sensitivity of the NR1(F639A) mutant to xenon and isoflurane is restored at low glycine concentrations. Although the F639A mutation causes a relatively modest change in the glycine affinity (presumably through an allosteric interaction), this can result in apparently different sensitivity of the receptor to anesthetics when wild-type and mutant receptors are studied at a fixed glycine concentration. The "reversal" of the effect of xenon and isoflurane in the mutant can be simply explained by the increased glycine affinity of the mutant, rather than reflecting a site where the anesthetics bind. Hence, our findings of competitive inhibition at the glycine site can account for the observations of Ogata *et al.*[30] In terms of competitive inhibition, we can think of anesthetics causing a parallel rightward shift in the glycine concentration–response curve, whereas the F639A mutation results in a compensatory leftward shift in the wild-type glycine concentration–response curve.

Interestingly, the F639A mutation was first identified as reducing inhibition of the NMDA receptor by ethanol.[6] Some studies of the effects of ethanol on NMDA receptors found that ethanol seemed competitive with glycine,[35,36] whereas others reported that ethanol was not competitive with glycine.[37,38] The reason for the discrepancy in these studies is not clear, and it remains to be resolved whether ethanol is competitive at the glycine site. Nevertheless, it is an interesting possibility that xenon, isoflurane, and ethanol may share a common site of action on the NMDA receptor.

Implications for General Anesthesia and Neuroprotection

Although other possible targets for xenon exist, such as two-pore domain potassium channels,[39] inhibition of NMDA receptors by xenon is likely to be involved in the action of xenon as an anesthetic and neuroprotectant. The role of NMDA receptors in anesthesia and neuroprotection by isoflurane is less clear. This has been partly due to conflicting reports in the literature as to the sensitivity of NMDA receptors to isoflurane and also because, unlike xenon, isoflurane significantly potentiates γ-aminobutyric acid type A receptors. While it remains likely that isoflurane's actions at the γ-aminobutyric acid type A receptor play a significant role in its action as an anesthetic, our finding that NMDA receptors can be sensitively inhibited by isoflurane indicate that inhibition of NMDA receptors by isoflurane may be involved in its action as an anesthetic and neuroprotectant.[40] Our finding that the inhibition by xenon and isoflurane is competitive with glycine at the NMDA receptor has important implications for general anesthesia and neuroprotection with these agents. Neuroprotective NMDA receptor glycine site antagonists, such as gavestinel, are well tolerated in patients and devoid of the psychotomimetic side effects common with some NMDA antagonists.[41] The mechanism of inhibition may play a role in the clinical profile. Because of the competitive nature of the inhibition, the degree of inhibition of NMDA receptors by xenon and isoflurane will depend

both on the glycine affinity of the receptors and on the glycine concentrations at the site of action in the CNS. Determining the concentration of glycine at NMDA receptors in the CNS is not trivial. Estimates of brain extracellular glycine concentrations, from microdialysis experiments, are around 5 μM.[42,43] However, the glycine concentrations at glutamatergic synapses may be much lower than this because of uptake by glycine transporters. There is strong evidence that glycine concentrations at synaptic NMDA receptors are significantly below saturating levels.[44] It is therefore possible that synaptic NMDA receptors may be more sensitive to inhibition by xenon and isoflurane than extrasynaptic receptors which are exposed to higher concentrations of glycine. However, in the case of xenon, the fact that there is also a component of noncompetitive inhibition means that even at saturating glycine concentrations, there is a significant degree of inhibition (approximately 30%). This noncompetitive component may be important in situations where there are likely to be elevated levels of agonist (such as ischemia). It may be that xenon's mixed competitive and noncompetitive inhibition of the NMDA receptor underlies its unique pharmacologic profile.

The authors thank Raquel Yustos, M.Sc. (Technician), for technical support, and Peter Brick, Ph.D. (Reader in Structural Biology), and Stephen Curry, Ph.D. (Professor of Structural Biology), for advice on PyMol (all from Imperial College London, London, United Kingdom).

Appendix: Clustering Analysis

Binding sites were determined *via* a clustering analysis which is similar to the method of Plotkin *et al.*[45] A trajectory file contains the positions and energies for each molecule at each stored step from the simulation. We define a "point" as the set of positions and energies for one molecule in one simulation step. The energy of the point is the energy of interaction of the gas molecule with the atoms of the protein and all of the other gas molecules in the system. Clusters are constructed based on the distances between points and on interaction energies.

We use a two-stage algorithm to avoid very large operation counts [$O(N^2)$]. In the first stage, clusters of molecule type j (*e.g.*, xenon) are determined by the following algorithm:

1. Assign the global minimum energy point for molecule type j to cluster $i = 1$.
2. Search through all the points of type j and create a sublist of those points whose position is within R_{max} of the minimum energy point for cluster i.
3. Iterate over the points in the sublist adding to the cluster those points whose position is within R_{test} of some other point already in cluster i.
4. Those points that are found to belong to cluster i are removed from the main list.
5. If the desired number of clusters have not been found, find the new global minimum energy point, assign it to cluster $i + 1$, and return to step 2.
6. All remaining points of type j are assigned to cluster 0 for bookkeeping purposes.

In the second stage, clusters-of-clusters or superclusters are determined which largely remove the dependence on the somewhat arbitrary parameter R_{max}. Two clusters that have any points within R_{test} of one another are merged to form a single supercluster. In this work, R_{max} = 3 Å and R_{test} = 1 Å were used. Note that a cluster as defined here is a property of the trajectory, not of the adsorbate density at a given time. A cluster potentially contains binding positions from all steps in the simulation and sometimes consists largely of many points representing different positions of a single adsorbate atom if it remains in one binding site as it moves throughout the simulation.

Using the minimum-energy points to identify the initial points for clusters focuses our interest on local energy minima as potential binding sites. Use of the R_{max} cutoff (R_{max} = 3 Å) incorporates the idea that a cluster of points will be associated with a physical binding site if it represents some small region of the protein. This also prevents the clustering algorithm's operation count from becoming $O(N^2)$, where N is the potentially very large number of points (all molecular positions for all steps) from the trajectory. The R_{test} criterion (R_{test} = 1 Å) incorporates the idea that we are looking for a region of space that would be continuously filled by mass points in the limit of long simulation runs and would be separated from other such regions by regions of low density where few or no molecules are adsorbed. As discussed by Plotkin *et al.*,[45] the value of R_{test} is related to a critical distance in continuum percolation theory and should be kept below the critical distance where essentially all points would be clustered together. The most appropriate value of R_{test} is a function of the length of the simulation, the fugacity or chemical potential of the gases treated *via* GCMC, and the number of configurations analyzed. The results presented here are, however, only a weak function of R_{test}. Similar clusters are identified with different values of R_{test}.

If more than one molecule type exists in the simulation (*e.g.*, xenon and water), our program also tests points corresponding to other molecule types for adherence to criterion 2, whereas criterion 3 is applied noniteratively to intermolecular distances between molecules of type j (*e.g.*, xenon) and molecules of the "other" types k (*e.g.*, water). Points of type k at position r_k are appended to a cluster i of type j if $|r_j - r_k| < R_{test}$ for any point of type j at r_j already in the cluster. For example, points corresponding to water molecules can be assigned to xenon clusters if they have positions within R_{test} of some xenon point already in the cluster and they also meet the R_{max} criterion. In this way, we can determine mixed occupancy of sites if it exists.

The first stage of the algorithm can be applied until every point is contained in a cluster (see step 5). For hydrated proteins with substantial amounts of otherwise empty space in the simulation cell, most xenon positions will lie in uninteresting and low-energy sites in these spaces relatively far from the protein. For the practical determination of relatively strongly bound sites, it is not necessary to assign all of these points to clusters and so we determine only a limited number of clusters, assigning the rest of the points to the background or "cluster 0." For the NMDA receptor, we report results from an assignment of 20 first-stage clusters. For the COMP test case (additional information regarding this is available on the ANESTHESIOLOGY Web site at http://www.anesthesiology.org), we assigned positions to 60 clusters.

References

1. Franks NP, Lieb WR: Molecular and cellular mechanisms of general anaesthesia. Nature 1994; 367:607–14
2. Yamakura T, Bertaccini E, Trudell JR, Harris RA: Anesthetics and ion channels: Molecular models and sites of action. Annu Rev Pharmacol Toxicol 2001; 41:23–51
3. Krasowski MD, Harrison NL: General anaesthetic actions on ligand-gated ion channels. Cell Mol Life Sci 1999; 55:1278–303
4. Franks NP: Molecular targets underlying general anaesthesia. Br J Pharmacol 2006; 147 (suppl 1):S72–81
5. Mihic SJ, Ye Q, Wick MJ, Koltchine VV, Krasowski MD, Finn SE, Mascia MP, Valenzuela CF, Hanson KK, Greenblatt EP, Harris RA, Harrison NL: Sites of alcohol and volatile anaesthetic action on GABA(A) and glycine receptors. Nature 1997; 389:385–9
6. Ronald KM, Mirshahi T, Woodward JJ: Ethanol inhibition of N-methyl-D-aspartate receptors is reduced by site-directed mutagenesis of a transmembrane domain phenylalanine residue. J Biol Chem 2001; 276:44729–35
7. Downie DL, Vicente-Agullo F, Campos-Caro A, Bushell TJ, Lieb WR, Franks

NP: Determinants of the anesthetic sensitivity of neuronal nicotinic acetylcholine receptors. J Biol Chem 2002; 277:10367–73

8. Mayer ML, Ghosal A, Dolman NP, Jane DE: Crystal structures of the kainate receptor GluR5 ligand binding core dimer with novel GluR5-selective antagonists. J Neurosci 2006; 26:2852–61

9. Furukawa H, Gouaux E: Mechanisms of activation, inhibition and specificity: Crystal structures of the NMDA receptor NR1 ligand-binding core. EMBO J 2003; 22:2873–85

10. Franks NP, Dickinson R, de Sousa SLM, Hall AC, Lieb WR: How does xenon produce anaesthesia? Nature 1998; 396:324

11. de Sousa SLM, Dickinson R, Lieb WR, Franks NP: Contrasting synaptic actions of the inhalational general anesthetics isoflurane and xenon. ANESTHESIOLOGY 2000; 92:1055–66

12. Wilhelm S, Ma D, Maze M, Franks NP: Effects of xenon on *in vitro* and *in vivo* models of neuronal injury. ANESTHESIOLOGY 2002; 96:1485–91

13. Resat H, Mezei M: Grand canonical ensemble Monte Carlo simulation of the dCpG/proflavine crystal hydrate. Biophys J 1996; 71:1179–90

14. Clark M, Guarnieri F, Shkurko I, Wiseman J: Grand canonical Monte Carlo simulation of ligand-protein binding. J Chem Inf Model 2006; 46:231–42

15. Hollmann MW, Liu HT, Hoenemann CW, Liu WH, Durieux ME: Modulation of NMDA receptor function by ketamine and magnesium: II. Interactions with volatile anesthetics. Anesth Analg 2001; 92:1182–91

16. Zhan X, Fahlman CS, Bickler PE: Isoflurane neuroprotection in rat hippocampal slices decreases with aging: Changes in intracellular Ca2+ regulation and N-methyl-D-aspartate receptor-mediated Ca2+ influx. ANESTHESIOLOGY 2006; 104:995–1003

17. Frenkel D, Smit B: Understanding Molecular Simulation. San Diego, Academic Press, 1996, pp 113–23

18. Reddy R, Erion MD, Agarwal A: Rev Computational Chem 2000; 16:217–88

19. Yang J, Ren Y, Tian A, Sun H: COMPASS force field for 14 inorganic molecules, He Ne, Ar, Kr, Xe, H_2, O_2, N_2, NO, CO, CO_2, NO_2, and SO_2 in liquid phases. J Phys Chem B 2000; 104:4951–7

20. Peterson BK, Valenzuela CA, Martin JCS, Franks NP: Adsorption simulations and biology: Grand canonical Monte Carlo calculations of binding locations, occupancy and free energies of xenon in COMP and mutant phage T4 lysozyme L99A. American Institute of Chemical Engineers Annual Meeting; 2005; Cincinnati, Ohio

21. Downie DL, Hall AC, Lieb WR, Franks NP: Effects of inhalational general anaesthetics on native glycine receptors in rat medullary neurones and recombinant glycine receptors in *Xenopus* oocytes. Br J Pharmacol 1996; 118:493–502

22. Cleland WW: The statistical analysis of enzyme kinetic data. Adv Enzymol Relat Areas Mol Biol 1967; 29:1–32

23. Franks NP, Lieb WR: Do general anaesthetics act by competitive binding to specific receptors? Nature 1984; 310:599–601

24. Curry S, Lieb WR, Franks NP: Effects of general anesthetics on the bacterial luciferase enzyme from Vibrio harveyi: An anesthetic target site with differential sensitivity. Biochemistry 1990; 29:4641–52

25. Malashkevich VN, Kammerer RA, Efimov VP, Schulthess T, Engel J: The crystal structure of a five-stranded coiled coil in COMP: A prototype ion channel? Science 1996; 274:761–5

26. Quillin ML, Breyer WA, Griswold IJ, Matthews BW: Size *versus* polarizability in protein-ligand interactions: Binding of noble gases within engineered cavities in phage T4 lysozyme. J Mol Biol 2000; 302:955–77

27. Sheng M, Cummings J, Roldan LA, Jan YN, Jan LY: Changing subunit composition of heteromeric NMDA receptors during development of rat cortex. Nature 1994; 368:144–7

28. Thomas CG, Miller AJ, Westbrook GL: Synaptic and extrasynaptic NMDA receptor NR2 subunits in cultured hippocampal neurons. J Neurophysiol 2006; 95:1727–34

29. Solt K, Eger EI II, Raines DE: Differential modulation of human N-methyl-D-aspartate receptors by structurally diverse general anesthetics. Anesth Analg 2006; 102:1407–11

30. Ogata J, Shiraishi M, Namba T, Smothers CT, Woodward JJ, Harris RA: Effects of anesthetics on mutant N-methyl-D-aspartate receptors expressed in *Xenopus* oocytes. J Pharmacol Exp Ther 2006; 318:434–43

31. Franks NP, Lieb WR: Temperature dependence of the potency of volatile general anesthetics: implications for *in vitro* experiments. ANESTHESIOLOGY 1996; 84:716–20

32. Yamakura T, Harris RA: Effects of gaseous anesthetics nitrous oxide and xenon on ligand-gated ion channels: Comparison with isoflurane and ethanol. ANESTHESIOLOGY 2000; 93:1095–101

33. Nishikawa K, MacIver MB: Excitatory synaptic transmission mediated by NMDA receptors is more sensitive to isoflurane than are non-NMDA receptor-mediated responses. ANESTHESIOLOGY 2000; 92:228–36

34. Dingledine R, Borges K, Bowie D, Traynelis SF: The glutamate receptor ion channels. Pharmacol Rev 1999; 51:7–61

35. Buller AL, Larson HC, Morrisett RA, Monaghan DT: Glycine modulates ethanol inhibition of heteromeric N-methyl-D-aspartate receptors expressed in *Xenopus* oocytes. Mol Pharmacol 1995; 48:717–23

36. Rabe CS, Tabakoff B: Glycine site-directed agonists reverse the actions of ethanol at the N-methyl-D-aspartate receptor. Mol Pharmacol 1990; 38:753–7

37. Mirshahi T, Woodward JJ: Ethanol sensitivity of heteromeric NMDA receptors: effects of subunit assembly, glycine and NMDAR1 Mg(2+)-insensitive mutants. Neuropharmacology 1995; 34:347–55

38. Peoples RW, Weight FF: Ethanol inhibition of N-methyl-D-aspartate-activated ion current in rat hippocampal neurons is not competitive with glycine. Brain Res 1992; 571:342–4

39. Gruss M, Bushell TJ, Bright DP, Lieb WR, Mathie A, Franks NP: Two-pore-domain K+ channels are a novel target for the anesthetic gases xenon, nitrous oxide, and cyclopropane. Mol Pharmacol 2004; 65:443–52

40. Bickler PE, Buck LT, Hansen BM: Effects of isoflurane and hypothermia on glutamate receptor-mediated calcium influx in brain slices. ANESTHESIOLOGY 1994; 81:1461–9

41. Dyker AG, Lees KR: Safety and tolerability of GV150526 (a glycine site antagonist at the N-methyl-D-aspartate receptor) in patients with acute stroke. Stroke 1999; 30:986–92

42. Kennedy RT, Thompson JE, Vickroy TW: *In vivo* monitoring of amino acids by direct sampling of brain extracellular fluid at ultralow flow rates and capillary electrophoresis. J Neurosci Methods 2002; 114:39–49

43. Dopico JG, Gonzalez-Hernandez T, Perez IM, Garcia IG, Abril AM, Inchausti JO, Rodriguez Diaz M: Glycine release in the substantia nigra: Interaction with glutamate and GABA. Neuropharmacology 2006; 50:548–57

44. Berger AJ, Dieudonne S, Ascher P: Glycine uptake governs glycine site occupancy at NMDA receptors of excitatory synapses. J Neurophysiol 1998; 80:3336–40

45. Plotkin JB, Chave J, Ashton PS: Cluster analysis of spatial patterns in Malaysian tree species. Am Naturalist 2002; 160:629–44